Appendix for

VRAC channel composition influences its substrate specificity and cellular resistance to Pt-based anti-cancer drugs

Rosa Planells-Cases, Darius Lutter, Charlotte Guyader, Nora M. Gerhards, Florian Ullrich, Deborah A. Elger, Asli Kucukosmanoglu, Guotai Xu, Felizia K. Voss, S. Momsen Reincke, Tobias Stauber, Vincent A. Blomen, Daniel J. Vis, Lodewyk F. Wessels, Thijn R. Brummelkamp, Piet Borst, Sven Rottenberg* and Thomas J. Jentsch*

*Corresponding authors. E-mail: Jentsch@fmp-berlin.de (T.J.J.); sven.rottenberg@vetsuisse.unibe.ch (S.R.)

Table of Contents

Appendix Figures

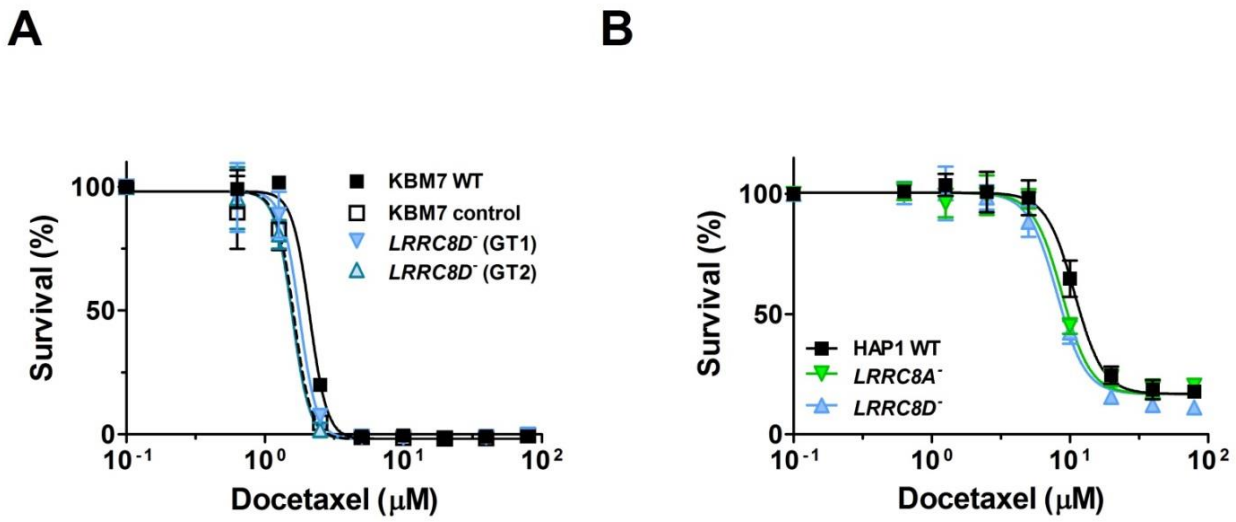

Appendix Figure S1. Docetaxel cytotoxicity assays of *LRRC8D*- or *LRRC8A*-deficient cells.

A. Survival (%) of parental, vector-transduced or *LRRC8D*-deficient GT1 and GT2 KBM7 cells exposed to increasing concentrations of docetaxel.

B. Survival of WT control, *LRRC8A*-, or *LRRC8D*-deficient HAP1 cells. n=3; error bars, standard deviation.

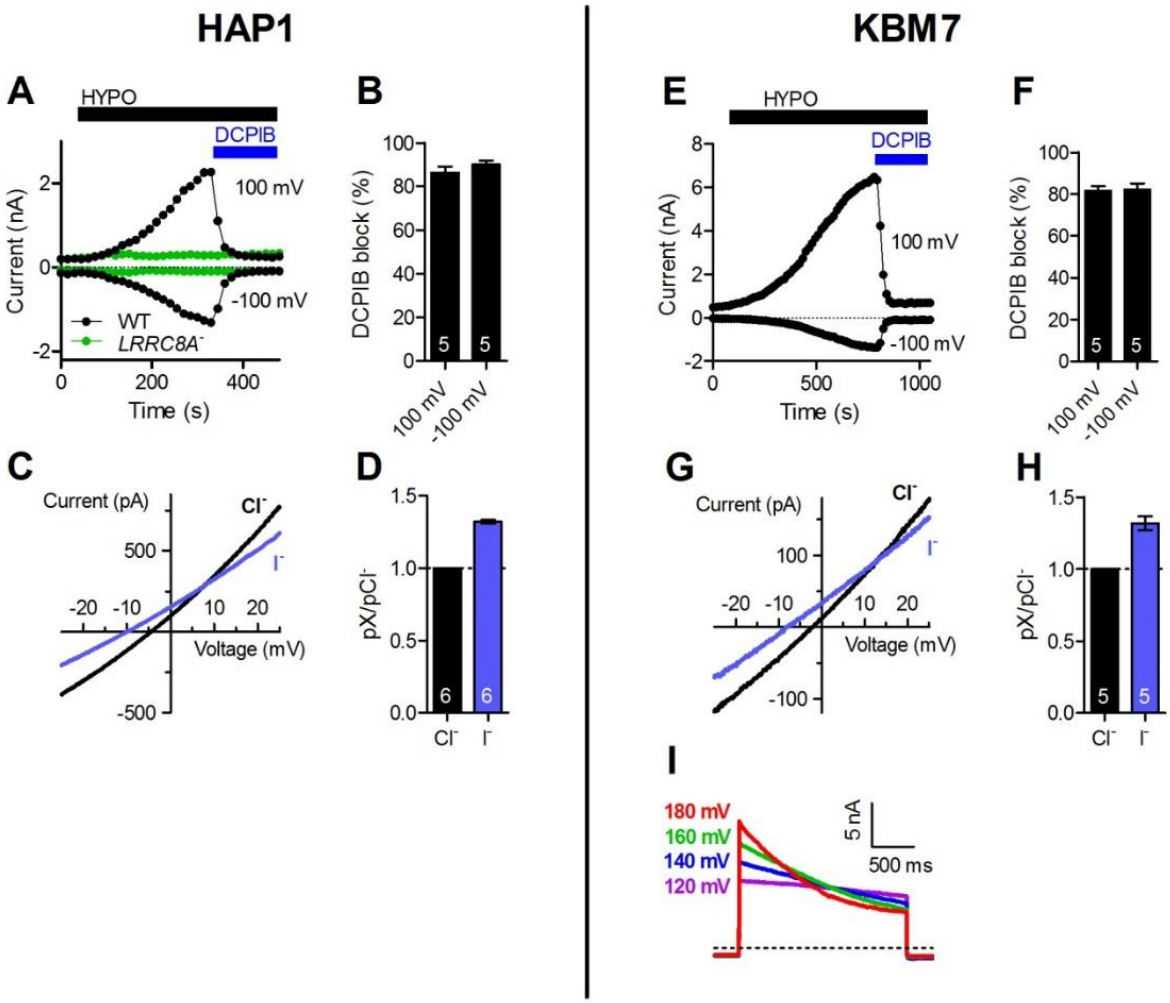

Appendix Figure S2. Characteristics of swelling-induced whole-cell currents recorded from HAP1 and KBM7 cells are consistent with $I_{Cl,vol}$.

A. Example of hypotonicity-activated currents in WT (black) and *LRRC8A*$^-$ (green) HAP1 cells at -100 mV and +100 mV registered every 15 s. Currents depended on LRRC8A and were rapidly inhibited by the VRAC inhibitor DCPIB (20 µM; TOCRIS).

B. Percentage of swelling-activated current in WT HAP1 cells at -100 mV and +100 mV blocked by 20 µM DCPIB.

C. Example current-voltage (I/V) relationships obtained from WT HAP1 cells at the time of maximal current activation with Cl^-- (black) and I^--containing (blue) hypotonic extracellular solutions. When Cl^- is substituted for I^-, the reversal potential shifts to the left, indicating the $I^- > Cl^-$ selectivity typical for $I_{Cl,vol}$.

D. Relative anion permeability (PX/PCl^-) as determined from shifts in reversal potential upon anion substitution (as seen in panel C). Relative permeabilities were calculated as described previously (Voss et al, 2014).

E. Example hypotonicity-activated currents in WT KBM7 cells at -100 mV and +100 mV registered every 15 s. Currents were rapidly inhibited by DCPIB (20 µM).

F. Percentage of swelling-activated current in KBM7 cells at -100 mV and +100 mV blocked by 20 µM DCPIB.

G. Example I/V relationships from WT KBM7 cells at the time of maximal activation with Cl- (black) and I--containing (blue) hypotonic extracellular solutions.

H. Relative anion permeability (PX/PCl^-) as determined from shifts in reversal potential upon anion substitution (as seen in panel G).

I. Example swelling-activated currents from KBM7 cells in response to the indicated voltages, displaying voltage-dependent inactivation at strongly depolarized potentials. The dashed line indicates zero current.

B,D,F,H, the number of cells is indicated on the bars. Error bars, SEM.

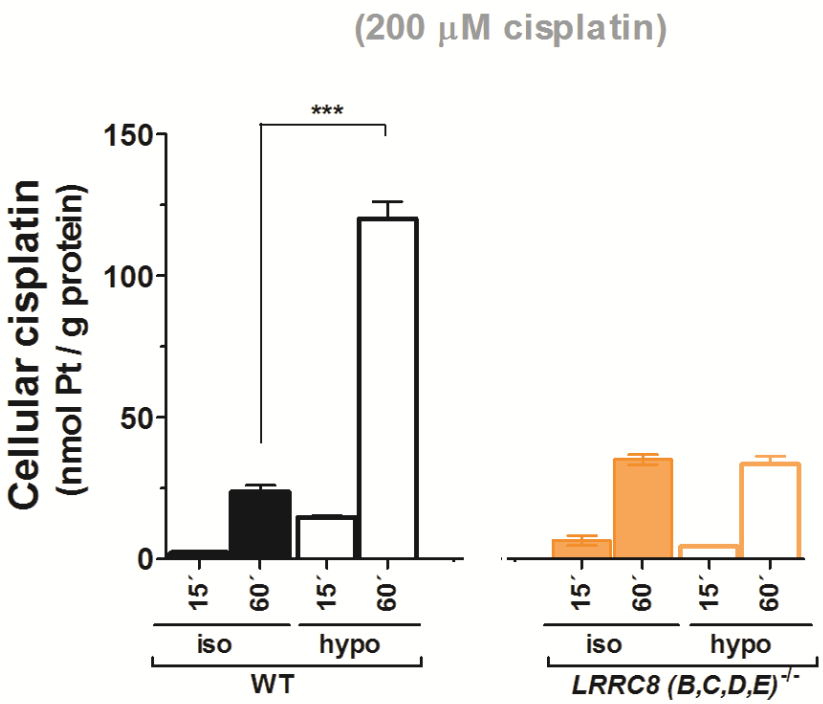

Appendix Figure S3. LRRC8 heteromers are required for cisplatin uptake.

Parallel disruption of LRRC8B-E abolishes swelling-activated cisplatin uptake (200 μM) into HCT116 cells, demonstrating that heteromers of LRRC8A with at least one other LRRC8 isoform are needed for uptake. Similar results were previously obtained for $I_{Cl,vol}$ (*1*). n=3; error bars, SEM. ***, p<0.001.

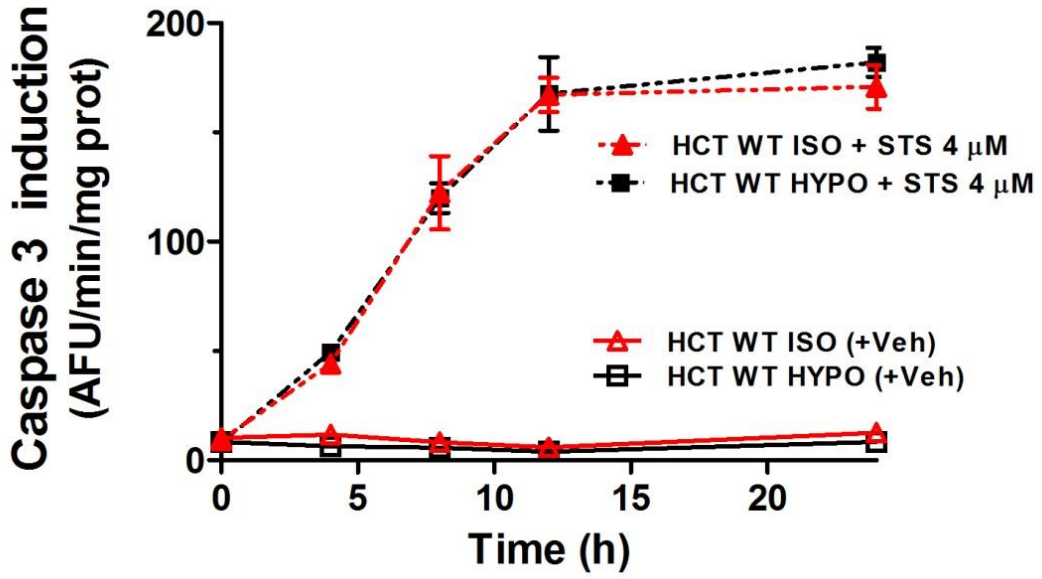

Appendix Figure S4. One-hour exposure to hypotonic solution did not induce caspase activity in HCT116 cells.

Exposure to 4 μM staurosporine for the same time induced caspase 3 irrespective of tonicity. Red and black lines correspond to cells treated for 1 h with isotonic- and hypotonic-saline, respectively (always containing 0.4% DMSO). Dotted lines correspond to cells exposed to staurosporine (STS) while solid lines denote vehicle-treated cells. AFU, arbitrary fluorescence units from enzymatic assay (see Methods). n=3; error bars, SEM.

Gene	Disruptive Insertions in Screen	Total Other Disruptive Insertions in Screen	Disruptive Insertions in Control	Total Other Disruptive Insertions in Control	p value	FDR-adjusted p value
LRRC8D	**49**	**1649**	**104**	**212574**	**8.0E-64**	**1.0E-60**
LRRC8A	**7**	**1691**	**11**	**212667**	**5.7E-11**	**3.6E-8**
MAP4K5	5	1693	17	212661	7.3E-07	0.0003
SEC24B	3	1695	4	212674	1.7E-05	0.004
SLFN11	4	1694	16	212662	1.7E-05	0.004

Appendix Table S1. Enrichment of gene-trap insertions in the population of KBM7 cells treated with carboplatin (screen) versus the control.

The number of insertion sites per gene and the total number of insertions of the carboplatin selected cells (screen) was compared to an unselected mutagenized population (control) as described previously (Carette et al, 2011). A one-sided Fisher exact test was used to calculate the p value. Correction for multiple testing for p values was carried out using the Benjamini and Hochberg FDR-correction.

	KBM7	KBM7 vector	*LRRC8D*^{GT1}	*LRRC8D*^{GT2}
Carboplatin				
IC50 (μM)	3.7	3.4	12.6	11.3
CI (95%)	2.5 - 5.5	2.1 - 5.5	7.3 - 22.0	6.3 - 20.3
Cisplatin				
IC50 (μM)	0.16	0.18	0.74	0.73
CI (95%)	0.10 - 0.26	0.11 - 0.29	0.48 - 1.144	0.43 - 1.22
Oxaliplatin				
IC50 (μM)	2.2	2.5	2.6	1.9
CI (95%)	1.2 – 3.7	1.6 – 4.0	1.7 – 3.7	1.3 – 2.7

Appendix Table S2. IC50 (average) and 95% confidence interval (CI) of the data presented in Fig. 1 for cisplatin, carboplatin and oxaliplatin.

Results were obtained from three independent experiments.

References

Carette JE, Guimarães CP, Wuethrich I, Blomen VA, Varadarajan M, Sun C, Bell G, Yuan B, Muellner MK, Nijman SM, Ploegh HL, Brummelkamp TR (2011) Global gene disruption in human cells to assign genes to phenotypes by deep sequencing. Nature biotechnology 29: 542-546

Voss FK, Ullrich F, Münch J, Lazarow K, Lutter D, Mah N, Andrade-Navarro MA, von Kries JP, Stauber T, Jentsch TJ (2014) Identification of LRRC8 heteromers as an essential component of the volume-regulated anion channel VRAC. Science 344: 634-638